Since January 2020 Elsevier has created a COVID-19 resource centre with free information in English and Mandarin on the novel coronavirus COVID-19. The COVID-19 resource centre is hosted on Elsevier Connect, the company's public news and information website.

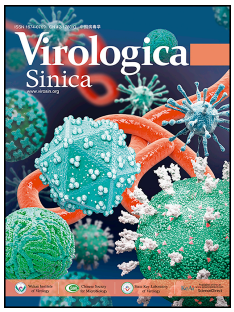

Neutralization of five SARS-CoV-2 variants of concern by convalescent and BBIBP-CorV vaccinee serum

Yuqi Zhu, Xinyi Yang, Jingna Xun, Jun Liu, Qing Wen, Yixiao Lin, Xiaoting Shen, Jun Chen, Songhua Yuan, Xiaying Zhao, Jing Wang, Hanyu Pan, Jinlong Yang, Zhiming Liang, Yue Liang, Qinru Lin, Huitong Liang, Min Li, Jianping Liu, Yinzhong Shen, Xiaoyan Zhang, Pengfei Wang, Daru Lu, Chunhua Yin, Jianqing Xu, Shibo Jiang, Hongzhou Lu, Huanzhang Zhu

PII: S1995-820X(22)00181-X

DOI: https://doi.org/10.1016/j.virs.2022.10.006

Reference: VIRS 122

To appear in: *Virologica Sinica*

Received Date: 25 July 2022

Accepted Date: 21 October 2022

Please cite this article as: Zhu, Y., Yang, X., Xun, J., Liu, J., Wen, Q., Lin, Y., Shen, X., Chen, J., Yuan, S., Zhao, X., Wang, J., Pan, H., Yang, J., Liang, Z., Liang, Y., Lin, Q., Liang, H., Li, M., Liu, J., Shen, Y., Zhang, X., Wang, P., Lu, D., Yin, C., Xu, J., Jiang, S., Lu, H., Zhu, H., Neutralization of five SARS-CoV-2 variants of concern by convalescent and BBIBP-CorV vaccinee serum, *Virologica Sinica*, https://doi.org/10.1016/j.virs.2022.10.006.

VS-6072
RESEARCH ARTICLE
Received: 25 July 2022, Accepted: 21 October 2022

Neutralization of five SARS-CoV-2 variants of concern by convalescent and BBIBP-CorV vaccinee serum

Yuqi Zhu [a], Xinyi Yang [a], Jingna Xun [a, b], Jun Liu [a, c], Qing Wen [a], Yixiao Lin [d], Xiaoting Shen [a], Jun Chen [d], Songhua Yuan [b], Xiaying Zhao [a], Jing Wang [a], Hanyu Pan [a], Jinlong Yang [a], Zhiming Liang [a], Yue Liang [a], Qinru Lin [a], Huitong Liang [a], Min Li[a] Jianping Liu [a], Yinzhong Shen [b], Xiaoyan Zhang [b], Pengfei Wang [a], Daru Lu [a],Chunhua Yin [a], Jianqing Xu [b], Shibo Jiang [e] , Hongzhou Lu [b, d, f, *], Huanzhang Zhu [a, *]

[a] State Key Laboratory of Genetic Engineering and Engineering Research Center of Gene Technology, Ministry of Education, Institute of Genetics, School of Life Sciences, Fudan University, Shanghai 200438, China
[b] Scientific Research Center, Shanghai Public Health Clinical Center, Fudan University, Shanghai 201508, China
[c] Fubio (Suzhou) Biomedical Technology Co., Ltd, Suzou 215300, China
[d] Department of Infectious Diseases and Immunology, Shanghai Public Health Clinical Center, Fudan University, Shanghai 201508, China
[e.] Key Laboratory of Medical Molecular Virology (MOE/NHC/CAMS), School of Basic Medical Sciences, Fudan University, Shanghai 200032, China
[f.] Department of Infectious Diseases and Nursing research institution, National Clinical Research Center for Infectious Diseases, The Third People's Hospital of Shenzhen , Shenzhen 518112, China.

***Corresponding authors**
E-mail address: hzzhu@fudan.edu.cn (H. Zhu); luhongzhou@fudan.edu.cn (H. Lu).
ORCID: 0000-0001-5797-0292 (H. Zhu); 0000-0002-8308-5534 (H. Lu)

Highlights

Pseudoviruses based on Alpha, Beta, Gamma, Delta and Omicron variants with GFP and luciferase reporter genes were constructed.

Delta and Omicron variant pseudoviruses exhibited higher infection rates than wild-type or other VOCs strains.

The neutralizing activity of vaccinee and convalescent serum against wild-type and VOCs weakened over-time.

Omicron variant more easily escaped the neutralization activity of convalescent and BBIBP-CorV vaccinee serum.

ABSTRACT

The prevalence of SARS-CoV-2 variants of concern (VOCs) is still escalating throughout the world. However, the level of neutralization of the inactivated viral vaccine recipients' sera and convalescent sera against all VOCs, including B.1.1.7 (Alpha), B.1.351 (Beta), P.1 (Gamma), B.1.617.2 (Delta), and B.1.1.529 (Omicron) remains to be lack of comparative analysis. Therefore, we constructed pseudoviruses of five VOCs using a lentiviral-based system and analyzed their viral infectivity and neutralization resistance to convalescent and BBIBP-CorV vaccinee serum at different times. Our results show that, compared with the wild-type strain (WT), five VOC pseudoviruses showed higher infection, of which B.1.617.2 and B.1.1.529 variant pseudoviruses exhibited higher infection rates than wild-type or other VOC strains, respectively. Sera from 10 vaccinated individuals at the 1, 3 and 5-month post second dose or from 10 convalescent in 14 and 200 days after discharge retained neutralizing activity against all strains but exhibited decreased neutralization activity significantly against the five VOC variant pseudoviruses over time compared to WT. Notably, 100% (30/30) of the vaccinee serum samples showed more than a 2.5-fold reduction in neutralizing activity against B.1.1.529, and 90% (18/20) of the convalescent serum samples showed more than 2.5-fold reduction in neutralization against B.1.1.529. These findings demonstrate the reduced protection against the VOCs in vaccinated and convalescent individuals over time, indicating that it is necessary to have a booster shot and develop new vaccines capable of eliciting broad neutralization antibodies.

Keywords: SARS-CoV-2; variants of concern (VOCs); convalescent; BBIBP-CorV vaccine; neutralization

1. Introduction

Since the first reports of severe acute respiratory syndrome coronavirus 2 (SARS-CoV-2) in humans in December 2019 (Wu et al., 2020; Zhou et al., 2020), numerous genetically distinct lineages have evolved (Harvey et al., 2021; Korber et al., 2020; Tao et al., 2021). Among those, the World Health Organization (WHO) reported that SARS-CoV-2 variants of concern (VOCs) associated with increased viral transmissibility and new waves of infection were constantly reported by WHO. Five SARS-CoV-2 VOCs have been identified since the beginning of the pandemic, including B.1.1.7 (Alpha) (Galloway et al., 2021; Volz et al., 2021), B.1.351 (Beta) (Tegally et al., 2021), P1 (Gamma) (Faria et al., 2021), B.1.617.2 (Delta) (Hetemaki et al., 2021) and B.1.1.529 (Omicron, BA.1), which is currently circulating (Callaway, 2021; WHO, 2021). These variants have multiple mutations in the genome, some of which are located on the spike protein. The B.1.1.7 variant includes 17 mutations in the viral genome. Of these, eight mutations (Δ69-70 deletion, Δ144 deletion, N501Y, A570D, P681H, T716I, S982A, D1118H) are in the spike protein (Galloway et al., 2021; Volz et al., 2021). The B.1.351 variant includes nine mutations (L18F, D80A, D215G, R246I, K417N, E484K, N501Y, D614G, and A701V) in the spike protein, of which three mutations (K417N, E484K, and N501Y) are located in the receptor-binding domain (RBD) and increase the binding affinity for the ACE receptors (Tegally et al., 2021). The P1 variant harbors eleven mutations in the spike protein (L18F, T20N, P26S, D138Y, R190S, H655Y, T1027I, V1176, K417T, E484K, and N501Y). Three mutations (L18F, K417N, E484K) are located in the RBD, similar to the B.1.351 variant (Faria et al., 2021). The B.1.617.2 variant harbors ten mutations (T19R, (G142D*), 156del, 157del, R158G, L452R, T478K, D614G, P681R, D950N) in the spike protein (Hetemaki et al., 2021). Omicron has by far the largest number of mutations among all SARS-CoV-2 variants. The reported mutations include N211del/L212I, Y145del, Y144del, Y143del, G142D, T95I, V70del, H69del, A67V in the N-terminal domain of the spike, Y505H, N501Y, Q498R, G496S, Q493R, E484A, T478K, S477N, G446S, N440K, K417N, S375F, S373P, S371L, G339D in the RBD of the spike, D796Y in the fusion peptide of the spike, L981F, N969K, Q954H in the heptad repeat 1 of the spike as well as multiple other mutations in the non-structural proteins and spike protein (Callaway, 2021; Daria et al., 2022; WHO, 2021).

These VOCs with mutations in the spike protein strongly influence SARS-CoV-2 transmission, antibody resistance, and vaccine efficacy. Because the spike protein is critical for viral entry, many mutations reside in the antigenic supersite in N-terminal domain (NTD) (Cerutti et al., 2021; Daria et al., 2022; McCallum et al., 2021) or the ACE2-binding site, a major target of potent virus-neutralizing antibodies (Piccoli et al., 2020). Indeed some groups have revealed that these variants are differentially resistant to the neutralizing antibodies elicited in convalescent and vaccinated individuals (Chen et al., 2021; Collier et al., 2021; Galloway et al., 2021; Garcia-Beltran et al., 2021; Greaney et al., 2021; Hoffmann et al., 2022, 2021; Liu J. et al., 2021; Liu Y. et al., 2021; Meng et al., 2022; Planas et al., 2021; Suzuki et al., 2022; Wang et al., 2021).

Although these recent studies evaluated the neutralization activities of some VOCs by convalescent and/or vaccine sera, up-to-date all five VOCs' neutralization resistance to the inactivated-virus vaccine and convalescent remains to lack a comparative analysis. Here, we, therefore, constructed six pseudotyped viruses displaying spike proteins derived from wild-type SARS-CoV-2, five VOCs including B.1.1.7 (Alpha), B.1.351 (Beta), P.1 (Gamma), B.1.617.2 (Delta) and B.1.1.529 (Omicron), and analyzed their infectivity in HEK293T cells expressing the ACE2 protein. We next compared this pseudovirus resistance to neutralization using sera obtained from ten vaccines at 1, 3 and 5-month after receipt of the second dose of inactivated-virus vaccines- BBIBP-CorV (Sinopharm, China), and from ten convalescents in 14 and 200 days after discharge.

2. Materials and methods

2.1 Bioinformatics

The wild-type SARS-CoV-2 whole genome sequences (WT, NC_045512.2) and variants (B.1.1.7, OV054768.1; B.1.351, OX003129.1; P.1, MZ477859.1; B.1.617.2, OK091006.1; B.1.1.529, OW996240.1) with related mutation

information downloaded from NCBI VIRUS (https://www.ncbi.nlm.nih.gov/labs/virus), which were aligned using alignment tools of NCBI, and a Maximum Likelihood phylogenetic tree was constructed using IQ-TREE Web Server(http://iqtree.cibiv.univie.ac.at/) (Trifinopoulos et al., 2016), employing the GTR as the substitution model and 1,000 bootstrap replications. Furthermore, mutations in the spike protein whose crystal structure complexed with ACE2 were obtained from the protein data bank (PDB ID: 7A98) (Benton et al., 2020) and were mapped using Biovia Discovery studio visualizer 2020.

2.2 Cells

HEK293T/17 was purchased from American Type Culture Collection (ATCC). The 293T-hACE2 cell line with high expression of human SARS-CoV-2 receptor ACE2 was previously generated in our lab. Huh-7 cells was purchased from Fubio Company (Suzhou, China). Cells were cultured in Dulbecco's Modified Eagle Medium (DMEM, HyClone, SH300243.01, USA) with 10% Fetal Bovine Serum (FBS, ExCell Bio, FSP500, China) and 1% penicillin/streptomycin (P/S, Gibco, cat.15140-122, USA) in a 37 °C incubator containing 5% CO_2. 0.25% Trypsin-EDTA (Gibco, cat.25200-056, USA) was used to digest cells for a subculture.

2.3 Human sera

Ten COVID-19 convalescent patients and ten BBIBP-CorV vaccinees were recruited from Shanghai Municipal Public Health center and Fudan University respectively. The basic information of volunteers was listed in Supplementary Table S1, including gender, age, disease severity, and sampling time interval. The study was approved by the School of Life Sciences at Fudan University (BE2001). For BBIBP-CorV vaccinees, the blood samples were obtained 1, 3, and 5 months after boosted the second vaccine. For COVID-19 convalescent patients, the blood sampling interval was according to the time of two follow-up visits after discharge. The first sampling time was nearly 14 days, and the second interval was nearly 200 days.

2.4 Construction and production of pseudoviruses

The spike segments of SARS-CoV-2 wild-type and five variants were synthesized by GeneScript Company (Nanjing, China) and inserted into pcDNA3.1 plasmid. All spike proteins were optimized with 18 amino acids removed and a HA tag attached. The pLenti.GFP.NLuc, which can express the green fluorescent protein (GFP) and luciferase simultaneously, was preserved by our laboratory. Plasmid psPAX2 was used for packaging the lentiviruses with pLenti.GFP.NLuc and the spike-pcDNA3.1.

HEK293T/17 cells were seeded into the 10 cm dishes, and grown to 80% confluence before transfection. The plasmids pLenti.GFP.NLuc, psPAX2, spike-pcDNA3.1 and Polyetherimide (PEI, Polysciences, cat.705149, USA) were added into the Optimal Minimal Essential Medium (Opti-MEM, Gibco, cat.2412271, USA) and mixed evenly, standing for 15 min, then were co-transfected into the HEK293T/17 cells. The culture medium was changed with 2% FBS and 1% P/S after incubation at 37 °C, 5% CO_2 for 24 h. The supernatants of the transfected cell containing SARS-CoV-2 pseudotyped viruses were harvested at 48 h and 72 h after transfection, filtered by 0.45 μm pore size (Merck Millipore, R1DB83053, USA). Then the filtrates were centrifuged at 125893×*g* 4 °C for 2 h (25,000 rpm, BeckmanCoulter, sw28, USA). The supernatants were discarded, and the pseudoviruses stocks were dissolved in Opti-MEM stored at −80 °C (Crawford et al., 2020; Hyseni et al., 2020; Riepler et al., 2020).

2.5 Titration of pseudoviruses

The titration of pseudoviruses was determined by HIV-1 Gag P24 DuoSet ELISA Kit (R&D, cat.7360-05, USA) according to the manufacturer's directions (Hyseni et al., 2020).

2.6 Infection assay

To measure the infectivity of pseudoviruses, 293T-hACE2 cells and Huh-7 cells (10^4 cells per well) were seeded at 96-well plates, and 3 μL [multiplicity of infection (MOI) = 0.3] of the pseudoviruses were added to each well with100 μL culture medium. Then the plates were incubated at 37 °C, 5% CO_2. After 12–16 h, the culture medium was refreshed, and the cells were cultured for another 48 h. The luciferase activity was measured by Luciferase reporter gene assay kit (Yeasen, cat.11401ES80, China) and SYNERGY2 microplate reader (BioTek, USA) to reflect the infectivity of pseudoviruses. .

2.7 Neutralization assay

The neutralization assay of pseudoviruses was performed as described previously (Chen et al., 2021; Wang et al., 2021). The 293T-hACE2 cells were seeded in a 96-well plate (1×10^4 cells per well) and cultured for 12 h. Serial dilutions of serum (starting at 1:40 dilution) were incubated with 3 μL (MOI = 0.3) of different SARS-CoV-2 pseudoviruses at 37 °C for 30 min before being adding to cells. Each dilution has three biology duplicates. Subsequently, the culture medium on cells was removed and 100 μL serum-pseudovirus mixture was added and incubated at 37 °C for 24 h. Then, the supernatant was discarded and cells were overlaid with fresh DMEM with 10% FBS and 1% P/S. After 48 h, chemiluminescence was measured by Luciferase reporter gene assay kit (Yeasen, cat.11401ES80, China). The ratio of the relative luminescence unit (RLU) of cells which added with serum-pseudovirus mixture and which infected with only pseudoviruses represented for the infectivity. The neutralization was calculated by (1–infectivity)%. The IC50 (50% inhibition concentration) values were calculated by a three-parameter dose-response-inhibition curve by transforming the dilutions to log10 in GraphPad Prism 8.

2.8 Quantification and statistical analysis

GraphPad Prism 8 was used for drawing plots and statistical analysis. All statistical tests were performed as described in the figure legends. The Fisher's precision probability test was performed as described the difference in IC50 between neutralizing antibodies against mutants. Nonlinear regression curve fitting was performed to calculate IC50 values. The *P*-value was less than 0.05 and was considered a statistically significant difference. **P* represented *P*-value was less than 0.05; ***P* represented *P*-value was less than 0.01; ****P* represented *P*-value was less than 0.001, *****P* represented *P*-value was less than 0.0001, ns represented there is no significant difference between each group. The statistical significance was calculated by t-test.

3. Results

3.1 Constructions of pseudotyped viruses related to variants

SARS-CoV-2 has undergone great diversification since the outbreak. WHO classified five lineages as the current VOCs, including B.1.1.7 (Alpha), B.1.351 (Beta), P.1 (Gamma), B.1.617.2 (Delta), and B.1.1.529 (Omicron). The genealogical evolution suggests that B.1.1.529 variant was derived from the B.1.1.7 variant, but there was a large discrepancy between them (**Fig. 1A**). All five reported VOCs have mutations in the RBD and the NTD. The variant B.1.1.529 has 34 mutations in spike protein. Some amino acid changes (Δ69/70, T95I, G142D, Δ145, K417N, T478K, N501Y, and P681H) are shared mutations also found in the Alpha, Beta, Gamma, or Delta VOCs. The ACE2 receptor interacted with the spike protein of five VOCs (**Fig. 1B**). To study the ability of immune evasion of the current VOCs, we constructed a total of six (five VOCs and WT) pseudoviruses that express spike proteins on lentivirus vectors (**Fig. 1C**), the titers of all pseudoviruses are adjusted to unity.

3.2 Infectivity of pseudoviruses related to five VOCs

To investigate the infectivity of pseudoviruses with VOCs spike protein, the level of relative luminescence activity was considered to reflect the infectivity. Different pseudoviruses were inoculated into the 293T-hACE2- and Huh-7 cells at the MOI of 0.3. Our findings showed that the five VOC variant pseudovirus displayed a 1.83–6.3 folds

increase in infectivity at 72 h post-infection in two cell lines compared to WT (**Fig. 1D**). Strikingly, B.1.617.2 and B.1.1.529 variants exhibited higher infection rates than wild-type or other VOCs variants. In contrast, no significant difference was found between the B.1.617.2 and B.1.1.529 variants in 293T-hACE2-, Huh-7 cells. These data suggest that mutants in the B.1.617.2 and B.1.1.529 variant promote viral entry into ACE2-expressing cells.

3.3 Reduced neutralization by vaccinee sera

To compare the neutralizing activity of antibodies induced by inactivated vaccines on WT and VOCs and to explore the effect of time on neutralizing activity, the neutralization experiments were conducted using a luciferase-expressing lentiviral pseudotyping system, and geometric mean titers (GMTs) were calculated to assess the neutralizing efficacy. The changes in neutralization sensitivity were quantitated by the mean of IC50. We accrued a cohort of 10 BBIBP-CorV vaccinees (**Supplement Table S1**). The entire cohort had a median age of 36 years (range: 22–56) and was 50% male. The serum samples were collected from vaccinated individuals at the 1-, 3-, and 5-months post the second dose of vaccination. The neutralization curves for vaccinated individuals are presented in **Fig. 2**. The result showed that sera from BBIBP-CorV vaccinee still have neutralizing activity against VOCs or WT five months after vaccination (**Fig. 2**).

The neutralization IC50 titers relative to the WT are quantified and tabulated as a fold increase or decrease (**Fig. 3A**). We found that the neutralizing activity of the vaccine serum against VOCswas decreased at the 1, 3, and 5-months after vaccination (**Fig. 2, Fig. 3A**). Noted that 100% (30/30) of the serum samples had more than a 2.5-fold reduction in neutralizing activity against B.1.1.529 variant, followed by P.1 (28/30, 93%), B.1.1.7 (26/30, 86%), B.1.617.2 (22/30, 73%), B.1.351 (20/30, 66%) (**Fig. 3A**). However, at one month after the second dose of vaccination, the IC50 of neutralizing activity against VOCs was reduced by 2.79-fold, 2.83-fold, 4.41-fold, 4.30-fold and 6.08-fold compared to WT , respectively. The IC50 of neutralizing activity against B.1.1.529 significantly decreased compared to other VOCs except P.1 (**Fig. 3B**).

Next, we compared the neutralizing activity of the same variant at different time points. We found that the IC50 of neutralizing activity against all VOCs and WT in the vaccinees' serum decreased significantly after five months post-vaccination (WT: 2.96-fold, B.1.1.7: 4.95-fold, B.1.351: 3.74-fold, P.1: 3.34-fold, B.1.617.2: 2.74-fold, and B.1.1.529: 4.97-fold (**Fig. 4**), A similar reduction of neutralizing activity was observed between the 1-month and 3-month or between the 3-month and 5-month's sera, respectively.

3.4 Reduced neutralization in COVID-19 convalescent sera

To evaluate the neutralizing activity of COVID-19 convalescent sera against the VOCs, the neutralization assays were conducted with WT and five VOCs. The serum samples of 10 convalescent volunteers infected with WT SARS-CoV-2 were obtained from the Shanghai Public Health Clinical Center at two different time points (an average of 14 days and 200 days after discharge) (**Supplement Table S1**). The entire cohort had a median age of 53 years (range: 33–68) and was 40% male with one severe case. The serum samples were also diluted for neutralization experiments. Similar to inactivated-virus vaccinee sera, we found that serum samples from all convalescent volunteers at 14 and 200 days after discharge maintained neutralizing activity against VOCs or WT (**Fig. 5**).

The results are summarized in **Fig. 6A** as a fold increase or decrease in serum neutralization IC50 titers. We found that compared with the WT, 90% percent (18/20) of the serum samples had more than a 2.5-fold reduction in neutralizing activity against B.1.1.529 variant, followed by 50% (10/20) B.1.351, 35% (7/20) P.1, 25% (5/20) B.1.1.7, 15% (3/20) B.1.617.2 (**Fig. 6A**). We found that the IC50 of neutralizing activity against B.1.1.7, B.1.351, P.1, B.1.617.2, and B.1.1.529 was reduced by 1.66-fold, 2.37-fold, 1.68-fold, 1.72-fold and 4.86-fold compared to WT at the time point of day 14, respectively (**Fig. 6B**). The IC50 of neutralizing activity against B.1.1.529 decreased significantly compared to other VOCs (**Fig. 6B**).

Finally, we analyzed the neutralizing activity of the same variant in the convalescent volunteers' sera from different

time points. We found that the IC50 of neutralizing activity against all VOCs and WT in the convalescent volunteers' sera decreased significantly over time (WT: 1.46-fold, B.1.1.7: 1.84-fold, B.1.351: 1.76-fold, P.1: 1.76-fold, B.1.617.2: 1.56-fold, and B.1.1.529: 1.81-fold) (**Fig. 7**). These data indicate that all VOCs escape from neutralizing antibodies in convalescent sera.

4. Discussion

SARS-CoV-2 VOCs have multiple mutations in the spike protein, which might alter important biological properties of the virus, including the efficiency of entry into target cells and the degree of vaccine protection. Here, we constructed five VOC-related pseudoviruses using a lentivirus-based system and systematically studied the effects of variants on virus infectivity and neutralization resistance to convalescent sera and inactivated-virus vaccine sera. Our findings showed that the VOC variant pseudoviruses displayed a 1.83–6.3 folds increase in infectivity at 72 h post-infection in two cell lines compared to WT. Strikingly, B.1.617.2 and B.1.1.529 variants exhibited higher infection rates than wild-type or other VOC strains, whereas no significant difference was found between the B.1.617.2 and B.1.1.529 variants in 293T-hACE2 and Huh-7 cells. These data suggest that mutants in the B.1.617.2 and B.1.1.529 variant promote viral entry into ACE2-expressing cells. Garcia-Beltran *et al*. reported that the Omicron pseudovirus continues to rely upon the human ACE2 receptor for target cell entry and infects target cells 4-fold more efficiently than wild-type pseudovirus and 2-fold more efficiently than Delta pseudovirus (Garcia-Beltran et al., 2022). The slightly inconsistent results of fold changes could be related to several factors, such as different infected cells (Mautner et al., 2022), virus titer, and time to assay after pseudovirus infection, but the trend of the infectivity is consistent.

In this study, our findings showed that sera from 10 vaccinated individuals at the 1-, 3- and 5-months post the second dose retained neutralizing activity against all VOC strains but the neutralization activity significantly decreased owing to the escape mutations and the waning of antibodies over time. Similar trends were also reported in other reports. Wang et al. reported an about 12.5-fold decrease of neutralization against the Omicron variant from recipients who received two doses of inactivated vaccine (Wang et al., 2022). In a population-based study of BNT162b2-vaccinated Africans, the vaccine-elicited neutralization against the Omicron variant shows a 22-fold reduction when compared with the ancestral SARS-CoV-2 strains (Cele et al., 2022).

Available evidence shows that the efficacy of major vaccines used worldwide against the VOCs are significantly dropped (Chen et al., 2021; Collier et al., 2021; Garcia-Beltran et al., 2022, 2021; Greaney et al., 2021; Hoffmann et al., 2022, 2021; J. Liu et al., 2021; Meng et al., 2022; Suzuki et al., 2022; X. Wang et al., 2022). Some studies showed a considerable decrease in the neutralizing potency of two doses of inactivated vaccines or RNA vaccines against Omicron (Cheng et al., 2022; Garcia-Beltran et al., 2022; Greaney et al., 2021; Hoffmann et al., 2022; Lu et al., 2021; Meng et al., 2022; Suzuki et al., 2022; X. Wang et al., 2022; Y. D. Wang et al., 2022; Zhang et al., 2022). The Omicron lineage of SARS-CoV-2 spread rapidly to become globally dominant and now has split into a number of sublineages including BA.1, BA.1.1, BA.2, BA.2.12.1, BA.2.75, BA.3, BA.4, and BA.5. Several recent studies showed that sera from individuals who received three doses of vaccines (Pfizer, AstraZeneca, or CoronaVac or BBIBP-CorV) have a reduced ability to neutralize BA.4, BA.5, and BA.2.75 compared with BA.1 (Ai et al., 2022; Cao et al., 2022; Tan et al., 2022; Tuekprakhon et al., 2022). These data suggest that BA.4, BA.5, and BA.2.75 subvariants can substantially escape neutralizing antibodies induced by vaccination. An Omicron-specific vaccine is advisable to developed, which expected to elicit neutralizing antibodies that help reduce the immune escape of Omicron strain.

Individuals exposed to SARS-CoV-2 produce antibodies, which display neutralization activity. Zhang *et al*. reported that the neutralization activity of convalescent sera against Omicron was reduced by 8.4-fold, whereas the neutralization activity of convalescent sera against other VOCs and VOIs was decreased by 1.2–4.5-fold compared to the D614G strain (Zhang et al., 2022). Wang *et al.* reported that 16 convalescent serum samples showed an average 10.5-fold reduction of neutralization against the Omicron variant when compared with the SARS-CoV-2 WT (Wang

et al., 2022). In another study, the neutralization activity of sera from ten convalescents showed a 32-fold drop against the Omicron variant compared to the WT SARS-CoV-2 (Liu et al., 2022). Consistent with these reports, we observed that sera of convalescents 14 and 200 days after discharge exhibited significant decrease neutralization activity against the VOC variant pseudoviruses compared to WT. All of these data revealed that the Omicron variant could easily escape the neutralization activity of convalescent sera.

5. Conclusions

In summary, we demonstrated that sera from vaccinated individuals at five months post the second dose of vaccination or convalescents at 200 days after discharge retained neutralizing activity against all SARS-CoV-2 strains. But both the vaccinated and convalescent individuals exhibited decreased neutralization activity against all VOCs, especially the Omicron variant, compared to WT. It is necessary to reveal the precise mechanisms through which a large number of mutations in the VOCs facilitate immune escape from the actions of neutralizing antibodies and develop new vaccines capable of eliciting broad neutralization antibodies.

Data availability

All the data generated during the current study are included in the manuscript.

Ethics Statement

This study was approved by the Ethics Committee of Shanghai Public Health Clinical Center and Fudan University. Written informed consent was obtained from the individual(s) for the publication of any potentially identifiable images or data included in this article. No animal experiments are involved.

Author Contributions

Yuqi Zhu: conceptualization, data curation, formal analysis, investigation, methodology, project administration, resources, software, validation, visualization, writing– original draft, writing – review & editing. Xinyi Yang: data curation, investigation. Jingna Xu: investigation, resources. Jun Liu: investigation. Qing Wen: visualization. Yixiao Lin: investigation, resources. Xiaoting Shen: investigation. Jun Chen: investigation, resources. Songhua Yuan: investigation, resources. Xiaying Zhao: investigation. Jing Wang: investigation. Hanyu Pan: investigation. Jinglong Yang: investigation. Zhiming Liang: investigation. Yue Liang: investigation. Qinru Lin: investigation. Huitong Liang: investigation. Min Li: investigation. Jianping Liu: supervision. Yinzhong Shen: supervision. Xiaoyan Zhang: supervision. Pengfei Wang: supervision, writing – review & editing. Daru Lu: supervision. Chunhua Yin: supervision. Jianqing Xu: supervision. Shibo Jiang: supervision. Hongzhou Lu: conceptualization, resources, supervision. Huanzhang Zhu: conceptualization, funding acquisition, project administration, supervision, review & editing.

Conflict of Interest

Author Jun Liu is employed by Fubio (Suzhou) Biomedical Technology Co., Ltd. The remaining authors declare that the research was conducted in the absence of any commercial or financial relationships that could be construed as a potential conflict of interest.

Acknowledgments

This work was supported by the National Natural Science Foundation of China (82041001, 81761128020). We also thank the State Key Laboratory of Genetic Engineering Fudan University, Shanghai Public Health Clinical Center, for providing the experimental platform and helping with sample collection.

Appendix A. Supplementary data

Supplementary data to this article can be found online at https://doi.org/10.1016/j.virs.####

Reference

Ai, J., Wang, X., He, X., Zhao, X., Zhang, Y., Jiang, Y., Li, M., Cui, Y., Chen, Y., Qiao, R., Li, L., Yang, L., Li, Y., Hu, Z., Zhang, W., Wang, P., 2022. Antibody evasion of SARS-CoV-2 Omicron BA.1, BA.1.1, BA.2, and BA.3 sub-lineages. Cell Host Microbe 30, 1077-1083.e4.

Benton, D.J., Wrobel, A.G., Xu, P., Roustan, C., Martin, S.R., Rosenthal, P.B., Skehel, J.J., Gamblin, S.J., 2020. Receptor binding and priming of the spike protein of SARS-CoV-2 for membrane fusion. Nature 588, 327–330.

Callaway, E., 2021. Heavily mutated Omicron variant puts scientists on alert. Nature 600, 21.

Cao, Y., Yisimayi, A., Jian, F., Song, W., Xiao, T., Wang, L., Du, S., Wang, J., Li, Q., Chen, X., Yu, Y., Wang, P., Zhang, Z., Liu, P., An, R., Hao, X., Wang, Yao, Wang, J., Feng, R., Sun, H., Zhao, L., Zhang, W., Zhao, D., Zheng, J., Yu, L., Li, C., Zhang, N., Wang, R., Niu, X., Yang, S., Song, X., Chai, Y., Hu, Y., Shi, Y., Zheng, L., Li, Z., Gu, Q., Shao, F., Huang, W., Jin, R., Shen, Z., Wang, Youchun, Wang, X., Xiao, J., Xie, X.S., 2022. BA.2.12.1, BA.4 and BA.5 escape antibodies elicited by Omicron infection. Nature 608, 593–602.

Cele, S., Jackson, L., Khoury, D.S., Khan, K., Moyo-Gwete, T., Tegally, H., San, J.E., Cromer, D., Scheepers, C., Amoako, D.G., Karim, F., Bernstein, M., Lustig, G., Archary, D., Smith, M., Ganga, Y., Jule, Z., Reedoy, K., Hwa, S.-H., Giandhari, J., Blackburn, J.M., Gosnell, B.I., Abdool Karim, S.S., Hanekom, W., von Gottberg, A., Bhiman, J.N., Lessells, R.J., Moosa, M.-Y.S., Davenport, M.P., de Oliveira, T., Moore, P.L., Sigal, A., 2022. Omicron extensively but incompletely escapes Pfizer BNT162b2 neutralization. Nature 602, 654–656.

Cerutti, G., Guo, Y.C., Zhou, T.Q., Gorman, J., Lee, M., Rapp, M., Reddem, E.R., Yu, J., Bahna, F., Bimela, J., Huang, Y.X., Katsamba, P.S., Liu, L.H., Nair, M.S., Rawi, R., Olia, A.S., Wang, P.F., Zhang, B.S., Chuang, G.Y., Ho, D.D., Sheng, Z.Z., Kwong, P.D., Shapiro, L., 2021. Potent SARS-CoV-2 neutralizing antibodies directed against spike N-terminal domain target a single supersite. Cell Host Microbe 29, 819-833.e7.

Chen, R.T.E., Zhang, X.W., Case, J.B., Winkler, E.S., Liu, Y., VanBlargan, L.A., Liu, J.Y., Errico, J.M., Xie, X.P., Suryadevara, N., Gilchuk, P., Zost, S.J., Tahan, S., Droit, L., Turner, J.S., Kim, W., Schmitz, A.J., Thapa, M., Wang, D. V, Boon, A.C.M., Presti, R.M., O'Halloran, J.A., Kim, A.H.J., Deepak, P., Pinto, D., Fremont, D.H., Crowe, J.E., Corti, D., Virgin, H.W., Ellebedy, A.H., Shi, P.Y., Diamond, M.S., 2021. Resistance of SARS-CoV-2 variants to neutralization by monoclonal and serum-derived polyclonal antibodies. Nat. Med. 27, 717–726.

Cheng, S.M.S., Mok, C.K.P., Leung, Y.W.Y., Ng, S.S., Chan, K.C.K., Ko, F.W., Chen, C.K., Yiu, K., Lam, B.H.S., Lau, E.H.Y., Chan, K.K.P., Luk, L.L.H., Li, J.K.C., Tsang, L.C.H., Poon, L.L.M., Hui, D.S.C., Peiris, M., 2022. Neutralizing antibodies against the SARS-CoV-2 Omicron variant BA.1 following homologous and heterologous CoronaVac or BNT162b2 vaccination. Nat. Med. 28, 486–489.

Collier, D.A., De Marco, A., Ferreira, I.A.T.M., Meng, B., Datir, R.P., Walls, A.C., Kemp, S.A., Bassi, J., Pinto, D., Silacci-Fregni, C., Bianchi, S., Tortorici, M.A., Bowen, J., Culap, K., Jaconi, S., Cameroni, E., Snell, G., Pizzuto, M.S., Pellanda, A.F., Garzoni, C., Riva, A., Elmer, A., Kingston, N., Graves, B., Mccoy, L.E., Smith, K.G.C., Bradley, J.R., Temperton, N., Ceron-Gutierrez, L., Barcenas-Morales, G., Harvey, W., Virgin, H.W., Lanzavecchia, A., Piccoli, L., Doffinger, R., Wills, M., Veesler, D., Corti, D., Gupta, R.K., BioResource, C.-N., UK, C.-19 G., 2021. Sensitivity of SARS-CoV-2 B.1.1.7 to mRNA vaccine-elicited antibodies. Nature 593, 136–141.

Crawford, K.H.D., Eguia, R., Dingens, A.S., Loes, A.N., Malone, K.D., Wolf, C.R., Chu, H.Y., Tortorici, M.A., Veesler, D., Murphy, M., Pettie, D., King, N.P., Balazs, A.B., Bloom, J.D., 2020. Protocol and reagents for pseudotyping lentiviral particles with SARS-CoV-2 spike protein for neutralization assays. Viruses 12, 513.

Daria, S., Bhuiyan, M.A., Islam, M.R., 2022. Detection of highly muted coronavirus variant Omicron (B.1.1.529) is triggering the alarm for South Asian countries: Associated risk factors and preventive actions. J. Med. Virol. 94, 1267–1268.

Faria, N.R., Mellan, T.A., Whittaker, C., Claro, I.M., Candido, D.D., Mishra, S., Crispim, M.A.E., Sales, F.C., Hawryluk, I., McCrone, J.T., Hulswit, R.J.G., Franco, L.A.M., Ramundo, M.S., de Jesus, J.G., Andrade, P.S., Coletti, T.M., Ferreira, G.M., Silva, C.A.M., Manuli, E.R., Pereira, R.H.M., Peixoto, P.S., Kraemer, M.U., Gaburo, N., Camilo, C.D., Hoeltgebaum, H., Souza, W.M., Rocha, E.C., de Souza, L.M., de Pinho, M.C., Araujo, L.J.T., Malta, F.S. V, de Lima, A.B., Silva, J.D., Zauli, D.A.G., Ferreira, A.C.D., Schnekenberg, R.P., Laydon, D.J., Walker, P.G.T., Schluter, H.M., dos Santos, A.L.P., Vidal, M.S., Del Caro, V.S., Filho, R.M.F., dos Santos, H.M., Aguiar, R.S., Proenca-Modena, J.L.P., Nelson, B., Hay, J.A., Monod, M., Miscouridou, X., Coupland, H., Sonabend, R., Vollmer, M., Gandy, A., Prete, C.A., Nascimento, V.H., Suchard, M.A., Bowden, T.A., Pond, S.L.K., Wu, C.H., Ratmann, O., Ferguson, N.M., Dye, C., Loman, N.J., Lemey, P., Rambaut, A., Fraiji, N.A., Carvalho, M.D.S.S., Pybus, O.G., Flaxman, S., Bhatt, S., Sabino, E.C., 2021. Genomics and epidemiology of the P.1 SARS-CoV-2 lineage in Manaus, Brazil. Science. 372, 815–821.

Galloway, S.E., Paul, P., MacCannell, D.R., Johansson, M.A., Brooks, J.T., MacNeil, A., Slayton, R.B., Tong, S., Silk,

B.J., Armstrong, G.L., Biggerstaff, M., Dugan, V.G., 2021. Emergence of SARS-CoV-2 B.1.1.7 Lineage - United States, December 29, 2020-January 12, 2021. MMWR Morb Mortal Wkly Rep 70, 95–99.

Garcia-Beltran, W.F., Lam, E.C., St Denis, K., Nitido, A.D., Garcia, Z.H., Hauser, B.M., Feldman, J., Pavlovic, M.N., Gregory, D.J., Poznansky, M.C., Sigal, A., Schmidt, A.G., Iafrate, A.J., Naranbhai, V., Balazs, A.B., 2021. Multiple SARS-CoV-2 variants escape neutralization by vaccine-induced humoral immunity. Cell 184, 2523.

Garcia-Beltran, W.F., St Denis, K.J., Hoelzemer, A., Lam, E.C., Nitido, A.D., Sheehan, M.L., Berrios, C., Ofoman, O., Chang, C.C., Hauser, B.M., Feldman, J., Roederer, A.L., Gregory, D.J., Poznansky, M.C., Schmidt, A.G., Iafrate, A.J., Naranbhai, V., Balazs, A.B., 2022. mRNA-based COVID-19 vaccine boosters induce neutralizing immunity against SARS-CoV-2 Omicron variant. Cell 185, 457-466.e4.

Greaney, A.J., Starr, T.N., Gilchuk, P., Zost, S.J., Binshtein, E., Loes, A.N., Hilton, S.K., Huddleston, J., Eguia, R., Crawford, K.H.D., Dingens, A.S., Nargi, R.S., Sutton, R.E., Suryadevara, N., Rothlauf, P.W., Liu, Z.M., Whelan, S.P.J., Carnahan, R.H., Crowe, J.E., Bloom, J.D., 2021. Complete Mapping of Mutations to the SARS-CoV-2 Spike Receptor-Binding Domain that Escape Antibody Recognition. Cell Host Microbe 29, 44-57.e9.

Harvey, W.T., Carabelli, A.M., Jackson, B., Gupta, R.K., Thomson, E.C., Harrison, E.M., Ludden, C., Reeve, R., Rambaut, A., Consortium, C.-G.U.K., Peacock, S.J., Robertson, D.L., 2021. SARS-CoV-2 variants, spike mutations and immune escape. Nat Rev Microbiol 19, 409–424.

Hetemaki, I., Kaariainen, S., Alho, P., Mikkola, J., Savolainen-Kopra, C., Ikonen, N., Nohynek, H., Lyytikainen, O., 2021. An outbreak caused by the SARS-CoV-2 Delta variant (B.1.617.2) in a secondary care hospital in Finland, May 2021. Euro Surveill 26, 2100636.

Hoffmann, M., Arora, P., Gross, R., Seidel, A., Hornich, B.F., Hahn, A.S., Kruger, N., Graichen, L., Hofmann-Winkler, H., Kempf, A., Winkler, M.S., Schulz, S., Jack, H.M., Jahrsdorfer, B., Schrezenmeier, H., Muller, M., Kleger, A., Munch, J., Pohlmann, S., 2021. SARS-CoV-2 variants B.1.351 and P.1 escape from neutralizing antibodies. Cell 184, 2384-2393.e12.

Hoffmann, M., Krüger, N., Schulz, S., Cossmann, A., Rocha, C., Kempf, A., Nehlmeier, I., Graichen, L., Moldenhauer, A.S., Winkler, M.S., Lier, M., Dopfer-Jablonka, A., Jäck, H.M., Behrens, G.M.N., Pöhlmann, S., 2022. The Omicron variant is highly resistant against antibody-mediated neutralization: Implications for control of the COVID-19 pandemic. Cell 185, 447-456.e11.

Hyseni, I., Molesti, E., Benincasa, L., Piu, P., Casa, E., Temperton, N.J., Manenti, A., Montomoli, E., 2020. Characterisation of SARS-CoV-2 Lentiviral Pseudotypes and Correlation between Pseudotype-Based Neutralisation Assays and Live Virus-Based Micro Neutralisation Assays. Viruses 12, 1011.

Korber, B., Fischer, W.M., Gnanakaran, S., Yoon, H., Theiler, J., Abfalterer, W., Hengartner, N., Giorgi, E.E., Bhattacharya, T., Foley, B., Hastie, K.M., Parker, M.D., Partridge, D.G., Evans, C.M., Freeman, T.M., de Silva, T.I., McDanal, C., Perez, L.G., Tang, H.L., Moon-Walker, A., Whelan, S.P., LaBranche, C.C., Saphire, E.O., Montefiori, D.C., Grp, S.C.-19 G., 2020. Tracking Changes in SARS-CoV-2 Spike: Evidence that D614G Increases Infectivity of the COVID-19 Virus. Cell 182, 812-827.e19.

Liu, J., Liu, Y., Xia, H., Zou, J., Weaver, S.C., Swanson, K.A., Cai, H., Cutler, M., Cooper, D., Muik, A., Jansen, K.U., Sahin, U., Xie, X., Dormitzer, P.R., Shi, P.Y., 2021. BNT162b2-elicited neutralization of B.1.617 and other SARS-CoV-2 variants. Nature 596, 273–275.

Liu, L.H., Iketani, S., Guo, Y.C., Chan, J.F.W., Wang, M., Liu, L.Y., Luo, Y., Chu, H., Huang, Y.M., Nair, M.S., Yu, J., Chik, K.K.H., Yuen, T.T.T., Yoon, C., To, K.K.W., Chen, H.L., Yin, M.T., Sobieszczyk, M.E., Huang, Y.X., Wang, H.H., Sheng, Z.Z., Yuen, K.Y., Ho, D.D., 2022. Striking antibody evasion manifested by the Omicron variant of SARS-CoV-2. Nature 602, 676–681.

Liu, Y., Liu, J., Xia, H., Zhang, X., Fontes-Garfias, C.R., Swanson, K.A., Cai, H., Sarkar, R., Chen, W., Cutler, M., Cooper, D., Weaver, S.C., Muik, A., Sahin, U., Jansen, K.U., Xie, X., Dormitzer, P.R., Shi, P.Y., 2021. Neutralizing Activity of BNT162b2-Elicited Serum. N Engl J Med 384, 1466–1468.

Lu, L., Mok, B.W.Y., Chen, L.L., Chan, J.M.C., Tsang, O.T.Y., Lam, B.H.S., Chuang, V.W.M., Chu, A.W.H., Chan, W.M., Ip, J.D., Chan, B.P.C., Zhang, R.Q., Yip, C.C.Y., Cheng, V.C.C., Chan, K.H., Jin, D.Y., Hung, I.F.N., Yuen, K.Y., Chen, H.L., To, K.K.W., 2021. Neutralization of Severe Acute Respiratory Syndrome Coronavirus 2 Omicron Variant by Sera From BNT162b2 or CoronaVac Vaccine Recipients. Clin. Infect. Dis. 75, e822–e826.

Mautner, L., Hoyos, M., Dangel, A., Berger, C., Ehrhardt, A., Baiker, A., 2022. Replication kinetics and infectivity of SARS-CoV-2 variants of concern in common cell culture models. Virol J 19, 76.

McCallum, M., De Marco, A., Lempp, F., Tortorici, M.A., Pinto, D., Walls, A.C., Beltramello, M., Chen, A., Liu, Z.M., Zatta, F., Zepeda, S., di Iulio, J., Bowen, J.E., Montiel-Ruiz, M., Zhou, J.Y., Rosen, L.E., Bianchi, S., Guarino, B., Fregni, C.S., Abdelnabi, R., Foo, S.Y.C., Rothlauf, P.W., Bloyet, L.M., Benigni, F., Cameroni, E., Neyts, J., Riva, A., Snell, G., Telenti, A., Whelan, S.P.J., Virgin, H.W., Corti, D., Pizzuto, M.S., Veesler, D., 2021. N-terminal domain antigenic mapping reveals a site of vulnerability for SARS-CoV-2. Cell 184, 2332-2347.e16.

Meng, B., Abdullahi, A., Ferreira, I.A.T.M., Goonawardane, N., Saito, A., Kimura, I., Yamasoba, D., Gerber, P.P., Fatihi,

S., Rathore, S., Zepeda, S.K., Papa, G., Kemp, S.A., Ikeda, T., Toyoda, M., Tan, T.S., Kuramochi, J., Mitsunaga, S., Ueno, T., Shirakawa, K., Takaori-Kondo, A., Brevini, T., Mallery, D.L., Charles, O.J., Bowen, J.E., Joshi, A., Walls, A.C., Jackson, L., Martin, D., Smith, K.G.C., Bradley, J., Briggs, J.A.G., Choi, J., Madissoon, E., Meyer, K.B., Mlcochova, P., Ceron-Gutierrez, L., Doffinger, R., Teichmann, S.A., Fisher, A.J., Pizzuto, M.S., de Marco, A., Corti, D., Hosmillo, M., Lee, J.H., James, L.C., Thukral, L., Veesler, D., Sigal, A., Sampaziotis, F., Goodfellow, I.G., Matheson, N.J., Sato, K., Gupta, R.K., 2022. Altered TMPRSS2 usage by SARS-CoV-2 Omicron impacts infectivity and fusogenicity. Nature 603, 706–714.

Piccoli, L., Park, Y.J., Tortorici, M.A., Czudnochowski, N., Walls, A.C., Beltramello, M., Silacci-Fregni, C., Pinto, D., Rosen, L.E., Bowen, J.E., Acton, O.J., Jaconi, S., Guarino, B., Minola, A., Zatta, F., Sprugasci, N., Bassi, J., Peter, A., De Marco, A., Nix, J.C., Mele, F., Jovic, S., Rodriguez, B.F., Gupta, S. V, Jin, F., Piumatti, G., Lo Presti, G., Pellanda, A.F., Biggiogero, M., Tarkowski, M., Pizzuto, M.S., Cameroni, E., Havenar-Daughton, C., Smithey, M., Hong, D., Lepori, V., Albanese, E., Ceschi, A., Bernasconi, E., Elzi, L., Ferrari, P., Garzoni, C., Riva, A., Snell, G., Sallusto, F., Fink, K., Virgin, H.W., Lanzavecchia, A., Corti, D., Veesler, D., 2020. Mapping Neutralizing and Immunodominant Sites on the SARS-CoV-2 Spike Receptor-Binding Domain by Structure-Guided High-Resolution Serology. Cell 183, 1024-1042.e21.

Planas, D., Bruel, T., Grzelak, L., Guivel-Benhassine, F., Staropoli, I., Porrot, F., Planchais, C., Buchrieser, J., Rajah, M.M., Bishop, E., Albert, M., Donati, F., Prot, M., Behillil, S., Enouf, V., Maquart, M., Smati-Lafarge, M., Varon, E., Schortgen, F., Yahyaoui, L., Gonzalez, M., De Seze, J., Pere, H., Veyer, D., Seve, A., Simon-Loriere, E., Fafi-Kremer, S., Stefic, K., Mouquet, H., Hocqueloux, L., van der Werf, S., Prazuck, T., Schwartz, O., 2021. Sensitivity of infectious SARS-CoV-2 B.1.1.7 and B.1.351 variants to neutralizing antibodies. Nat Med 27, 917–924.

Riepler, L., Rössler, A., Falch, A., Volland, A., Borena, W., Kimpel, J., von Laer, D., 2020. Comparison of four SARS-CoV-2 neutralization assays. Vaccines 9, 13. https://doi.org/10.3390/vaccines9010013

Suzuki, R., Yamasoba, D., Kimura, I., Wang, L., Kishimoto, M., Ito, J., Morioka, Y., Nao, N., Nasser, H., Uriu, K., Kosugi, Y., Tsuda, M., Orba, Y., Sasaki, M., Shimizu, R., Kawabata, R., Yoshimatsu, K., Asakura, H., Nagashima, M., Sadamasu, K., Yoshimura, K., Sawa, H., Ikeda, T., Irie, T., Matsuno, K., Tanaka, S., Fukuhara, T., Sato, K., G2P-Japan, G.P.J., 2022. Attenuated fusogenicity and pathogenicity of SARS-CoV-2 Omicron variant. Nature 603, 700–705.

Tan, C.-W., Lim, B.-L., Young, B.E., Yeoh, A.Y.-Y., Yung, C.-F., Yap, W.-C., Althaus, T., Chia, W.-N., Zhu, F., Lye, D.C., Wang, L.-F., 2022. Comparative neutralisation profile of SARS-CoV-2 omicron subvariants BA.2.75 and BA.5. The Lancet. Microbe.

Tao, K., Tzou, P.L., Nouhin, J., Gupta, R.K., de Oliveira, T., Kosakovsky Pond, S.L., Fera, D., Shafer, R.W., 2021. The biological and clinical significance of emerging SARS-CoV-2 variants. Nat Rev Genet 22, 757–773.

Tegally, H., Wilkinson, E., Giovanetti, M., Iranzadeh, A., Fonseca, V., Giandhari, J., Doolabh, D., Pillay, S., San, E.J., Msomi, N., Mlisana, K., von Gottberg, A., Walaza, S., Allam, M., Ismail, A., Mohale, T., Glass, A.J., Engelbrecht, S., Van Zyl, G., Preiser, W., Petruccione, F., Sigal, A., Hardie, D., Marais, G., Hsiao, N.Y., Korsman, S., Davies, M.A., Tyers, L., Mudau, I., York, D., Maslo, C., Goedhals, D., Abrahams, S., Laguda-Akingba, O., Alisoltani-Dehkordi, A., Godzik, A., Wibmer, C.K., Sewell, B.T., Lourenco, J., Alcantara, L.C.J., Kosakovsky Pond, S.L., Weaver, S., Martin, D., Lessells, R.J., Bhiman, J.N., Williamson, C., de Oliveira, T., 2021. Detection of a SARS-CoV-2 variant of concern in South Africa. Nature 592, 438–443.

Trifinopoulos, J., Nguyen, L.T., von Haeseler, A., Minh, B.Q., 2016. W-IQ-TREE: a fast online phylogenetic tool for maximum likelihood analysis. Nucleic Acids Res. 44, W232-5.

Tuekprakhon, A., Nutalai, R., Dijokaite-Guraliuc, A., Zhou, D., Ginn, H.M., Selvaraj, M., Liu, C., Mentzer, A.J., Supasa, P., Duyvesteyn, H.M.E., Das, R., Skelly, D., Ritter, T.G., Amini, A., Bibi, S., Adele, S., Johnson, S.A., Constantinides, B., Webster, H., Temperton, N., Klenerman, P., Barnes, E., Dunachie, S.J., Crook, D., Pollard, A.J., Lambe, T., Goulder, P., Paterson, N.G., Williams, M.A., Hall, D.R., Fry, E.E., Huo, J., Mongkolsapaya, J., Ren, J., Stuart, D.I., Screaton, G.R., 2022. Antibody escape of SARS-CoV-2 Omicron BA.4 and BA.5 from vaccine and BA.1 serum. Cell 185, 2422-2433.e13.

Volz, E., Mishra, S., Chand, M., Barrett, J.C., Johnson, R., Geidelberg, L., Hinsley, W.R., Laydon, D.J., Dabrera, G., Toole, A.O., Amato, R., Ragonnet-Cronin, M., Harrison, I., Jackson, B., Ariani, C. V, Boyd, O., Loman, N.J., McCrone, J.T., Goncalves, S., Jorgensen, D., Myers, R., Hill, V., Jackson, D.K., Gaythorpe, K., Groves, N., Sillitoe, J., Kwiatkowski, D.P., Flaxman, S., Ratmann, O., Bhatt, S., Hopkins, S., Gandy, A., Rambaut, A., Ferguson, N.M., Consor, C.-19 G.U.K.C.-U., 2021. Assessing transmissibility of SARS-CoV-2 lineage B.1.1.7 in England. Nature 593, 266–269.

Wang, P.F., Nair, M.S., Liu, L.H., Iketani, S., Luo, Y., Guo, Y.C., Wang, M., Yu, J., Zhang, B.S., Kwong, P.D., Graham, B.S., Mascola, J.R., Chang, J.Y., Yin, M.T., Sobieszczyk, M., Kyratsous, C.A., Shapiro, L., Sheng, Z.Z., Huang, Y.X., Ho, D.D., 2021. Antibody resistance of SARS-CoV-2 variants B.1.351 and B.1.1.7. Nature 593, 130–135.

Wang, X., Zhao, X.Y., Song, J.Y., Wu, J., Zhu, Y.Q., Li, M.H., Cui, Y.C., Chen, Y.J., Yang, L.L., Liu, J., Zhu, H.Z., Jiang,

S.B., Wang, P.F., 2022. Homologous or heterologous booster of inactivated vaccine reduces SARS-CoV-2 Omicron variant escape from neutralizing antibodies. Emerg. Microbes Infect. 11, 477–481.

Wang, Y.D., Ma, Y.P., Xu, Y., Liu, J.Y., Li, X., Chen, Y.Y., Chen, Y., Xie, J., Xiao, L.B., Xiang, Z., Wu, F., Huang, J.H., 2022. Resistance of SARS-CoV-2 Omicron variant to convalescent and CoronaVac vaccine plasma. Emerg. Microbes Infect. 11, 424–427.

WHO, 2021. Classification of Omicron (B.1.1.529): SARS-CoV-2 Variant of Concern [WWW Document]. URL https://www.who.int/news/item/26-11-2021-classification-of-omicron-(b.1.1.529)-sars-cov-2-variant-of-concern (Accessed 11.26.21).

Wu, F., Zhao, S., Yu, B., Chen, Y.M., Wang, W., Song, Z.G., Hu, Y., Tao, Z.W., Tian, J.H., Pei, Y.Y., Yuan, M.L., Zhang, Y.L., Dai, F.H., Liu, Y., Wang, Q.M., Zheng, J.J., Xu, L., Holmes, E.C., Zhang, Y.Z., 2020. Author Correction: A new coronavirus associated with human respiratory disease in China. Nature 579, 265–269.

Zhang, L., Li, Q.Q., Wu, J.J., Yu, Y.L., Zhang, Y., Nie, J.H., Liang, Z.T., Cui, Z.M., Liu, S., Wang, H.X., Ding, R.X., Jiang, F., Li, T., Nie, L.L., Lu, Q., Li, J.Y., Qin, L.L., Jiang, Y.N., Shi, Y., Xu, W.B., Huang, W.J., Wang, Y.C., 2022. Analysis of SARS-CoV-2 variants B.1.617: host tropism, proteolytic activation, cell-cell fusion, and neutralization sensitivity. Emerg. Microbes Infect. 11, 1024–1036.

Zhou, P., Yang, X.L., Wang, X.G., Hu, B., Zhang, L., Zhang, W., Si, H.R., Zhu, Y., Li, B., Huang, C.L., Chen, H.D., Chen, J., Luo, Y., Guo, H., Jiang, R.D., Liu, M.Q., Chen, Y., Shen, X.R., Wang, X., Zheng, X.S., Zhao, K., Chen, Q.J., Deng, F., Liu, L.L., Yan, B., Zhan, F.X., Wang, Y.Y., Xiao, G.F., Shi, Z.L., 2020. Addendum: A pneumonia outbreak associated with a new coronavirus of probable bat origin. Nature 579, 270–273.

Figure legend

Fig. 1. Identified SARS-CoV-2 variants. **A** Phylogenetic tree of SARS-CoV-2 VOC. **B** Spike protein diagram of B.1.1.7, B.1.351, P.1, B.1.617.2, B.1.1.529 strain. Different point mutation positions are marked and displayed with ACE2 receptor. **C** Mutations in the viral spike identified in B.1.1.7, B.1.351, P.1, B.1.617.2, B.1.1.529 strain and the corresponding mutation sites. **D** The infectivity of pseudoviruses in 293T-hACE2 cells and Huh-7 cells reflected by relative luminescence unit (RLU). Cells were infected with pseudoviruses and the luminescence activity was measured at 72 hours post-infection. The ratios of RLU in variants groups compared to WT were marked on the top of bars. All experiments had three duplications independently (mean ± SEM).

Fig. 2. Neutralization capability of sera from vaccinees at three different time posts post vaccination. Sera samples were collected from ten vaccinees (V001–V010) at the 1-, 3- and 5-months post the second dose of vaccination. The neutralization activity of sera against WT and VOC pseudoviruses was determined by neutralization assay. All data were obtained from three independent experiments (mean ± SEM). The X axis is log10 to represent the sera dilution ratio, and the Y axis is to represent the ability of neutralization of serum.

Fig. 3. The comparison of resistance of SARS-CoV-2 variants to inactivated vaccine sera. **A** The fold changes in neutralization activity of vaccine sera were shown in the ratio of IC50 between the variant and WT SARS-CoV-2 ($IC50_{\text{WT SARS-CoV-2}}/IC50_{\text{variant SARS-CoV-2}}$) as a heatmap with darker color implying greater change (≥2.5-fold). **B** The comparison of neutralization activity of sera from ten vaccinees (V001–V010) at one month post the second dose of vaccination against different variants. The IC50 (50% inhibition concentration) values were calculated by a three-parameter dose-response-inhibition curve. All data were obtained from three independent experiments (mean ± SEM). Mean fold changes in IC50 values are denoted above the *P* values. Statistical analysis was performed using a ratio paired *t*-test. ***$P < 0.001$; **** $P <$ 0001.

Fig. 4. The comparison of neutralization activity of vaccinees sera against the same variant at 1-, 3- and 5-mouths post vaccination. All data were obtained from three independent experiments (mean ± SEM). Mean fold changes in IC50 values are denoted above the *P* values. Statistical analysis was performed using a paired *t*-test. *$P < 0.05$; **$P < 0.01$; *** $P < 0.001$; **** $P < 0.0001$.

Fig. 5. Neutralization capability of sera from convalescents at 14 days and 200 days after discharge. Sera samples were collected from ten convalescents (P001–P010) at 14 days and 200 days after discharge. The neutralization activity of sera against WT and VOC pseudoviruses was determined by neutralization assay. All data were obtained from three independent experiments (mean ± SEM). P007* is a severe case. The X axis is log10 to represent the plasma dilution ratio, and the Y axis is to represent the ability of neutralization of serum.

Fig. 6. The comparison of resistance of SARS-CoV-2 variants to convalescent sera. **A** The fold changes in neutralization activity of convalescent sera were shown in the ratio of IC50 between the variant and WT SARS-CoV-2 ($IC50_{\text{WT SARS-CoV-2}}/IC50_{\text{variant SARS-CoV-2}}$) as a heatmap with darker color implying greater change (≥2.5-fold). P007* is a severe case. **B** The comparison of neutralization activity of sera from convalescents (P001–P010) at 14 days after discharge. All data were obtained from three independent experiments (mean±SEM). Mean fold changes in IC50 values are denoted above the *P*

values. Statistical analysis was performed using a ratio paired *t*-test. *$P < 0.05$; **$P < 0.01$.

Fig. 7. The comparison of neutralization activity of convalescents' sera against the same variant at different phases after discharge. All data were obtained from three independent experiments (mean ± SEM). Mean fold changes in IC50 values are denoted above the *P* values. Statistical analysis was performed using a paired *t*-test. *$P < 0.05$; **$P < 0.01$; *** $P < 0.001$.

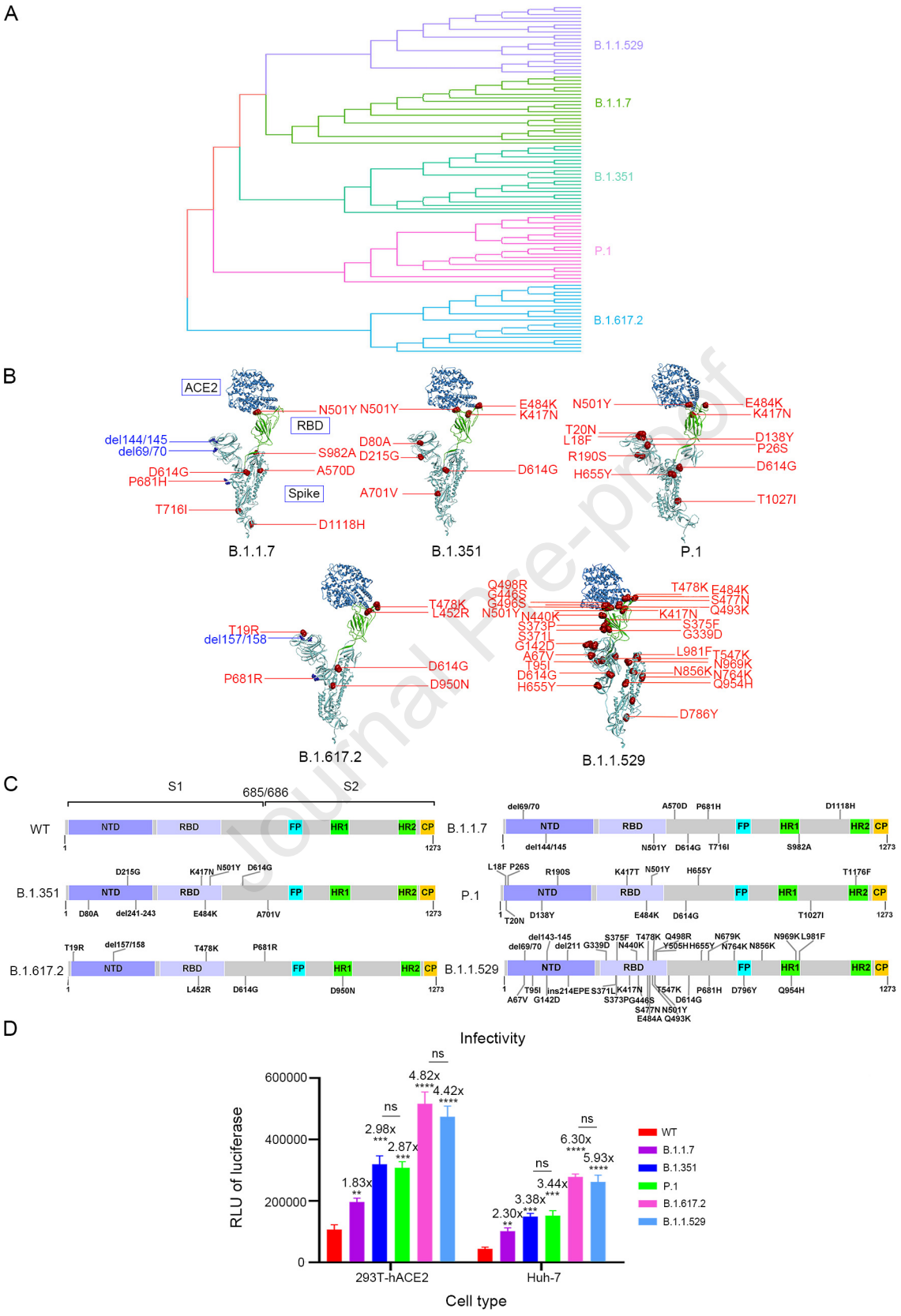

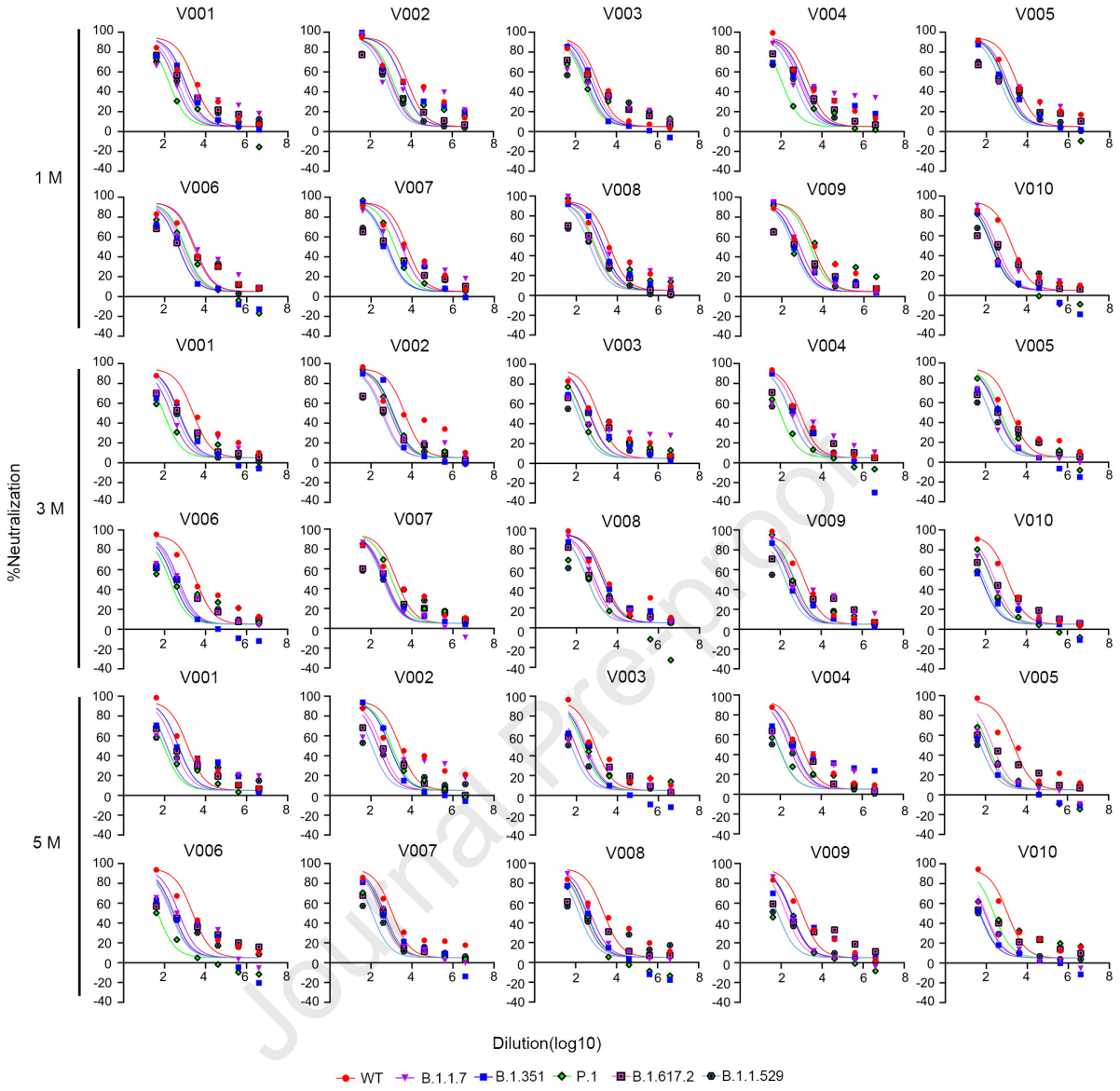

A

Fold change	IC50 of WT / IC50 of Variants														
	WT/B.1.1.7			WT/B.1.351			WT/P.1			WT/B.1.617.2			WT/B.1.1.529		
Volunteer	1 M	3 M	5 M	1 M	3 M	5 M	1 M	3 M	5 M	1 M	3 M	5 M	1 M	3 M	5 M
V01	7.89	9.78	9.99	2.38	3.75	2.74	13.83	20.99	12.76	3.85	5.19	5.97	6.58	7.07	12.88
V02	6.13	3.85	9.66	1.50	2.65	1.86	4.04	3.22	1.57	5.25	5.16	3.05	7.69	6.06	9.33
V03	3.58	4.97	9.01	1.64	2.17	3.19	4.16	4.64	4.33	1.25	1.26	1.55	2.56	4.82	8.98
V04	2.69	3.60	4.46	2.18	1.50	2.13	14.84	8.56	11.23	1.95	1.58	1.83	4.23	2.97	9.01
V05	3.59	9.47	19.61	3.57	4.12	32.88	3.78	2.85	15.59	3.62	2.42	3.88	5.47	6.42	14.91
V06	1.13	7.18	5.02	5.11	12.98	9.15	2.68	25.21	41.24	3.92	6.14	6.65	3.09	5.33	7.53
V07	1.71	2.45	2.13	8.05	2.82	2.69	3.39	1.33	2.59	8.85	3.99	5.42	10.47	4.43	14.73
V08	3.36	2.85	2.88	1.84	1.25	4.51	4.82	6.89	5.71	5.11	3.29	4.42	8.26	5.64	7.44
V09	3.21	3.05	3.03	4.83	4.53	3.17	3.87	4.11	15.39	5.79	4.16	2.42	7.19	8.66	6.25
V10	6.89	5.72	11.77	9.24	16.48	19.52	8.63	5.85	5.31	6.36	5.19	9.06	6.44	17.17	16.41

– +

B

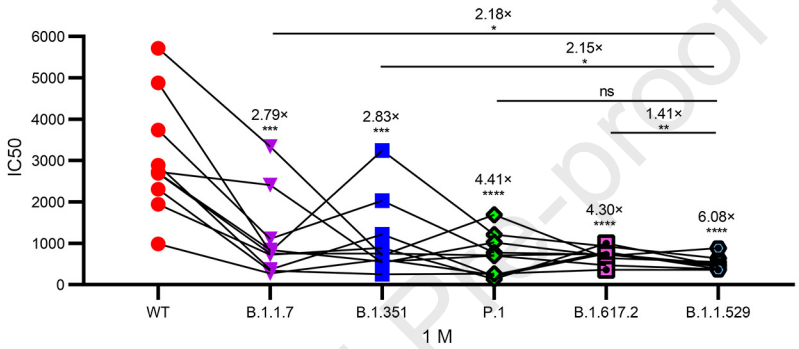

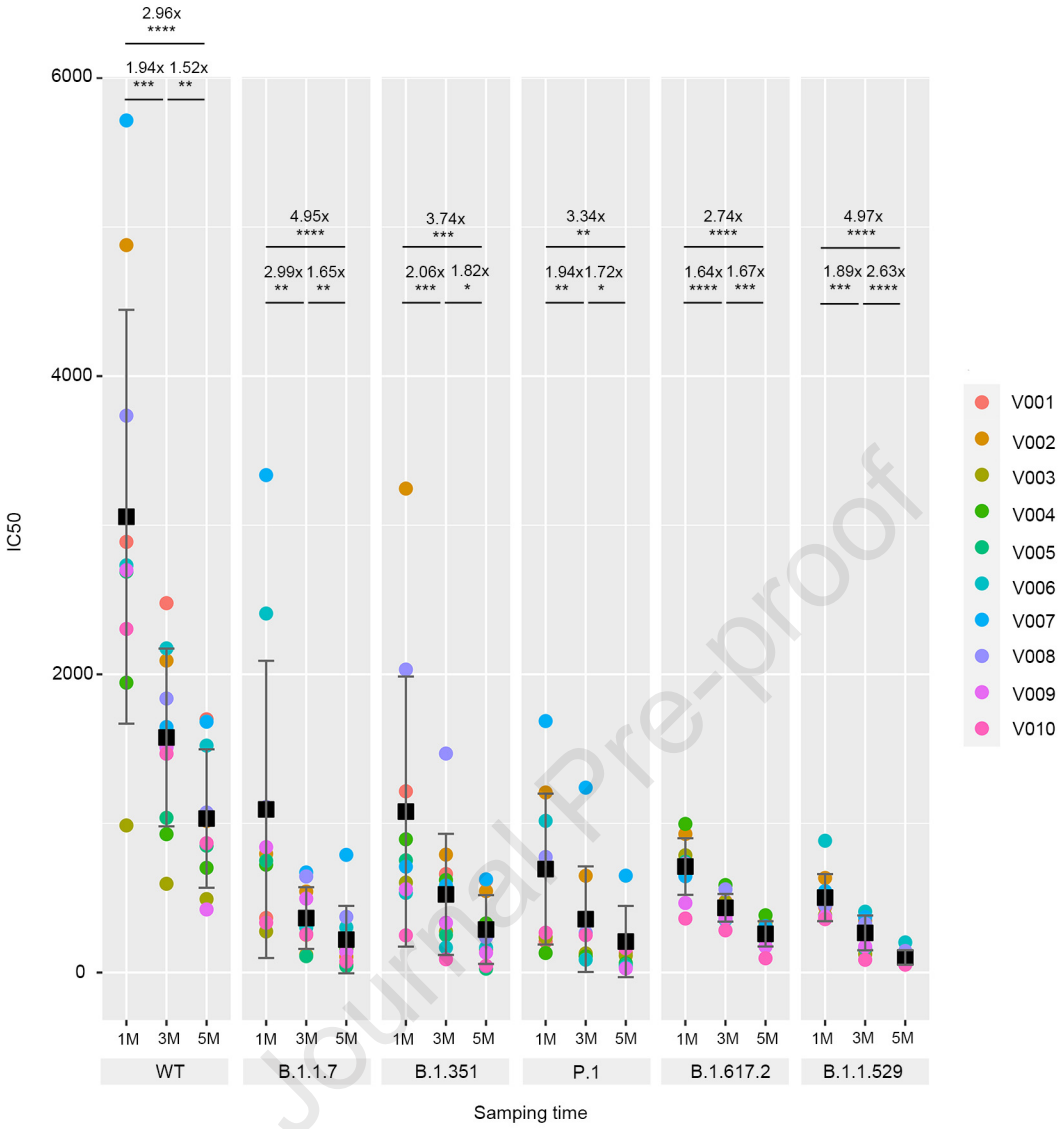

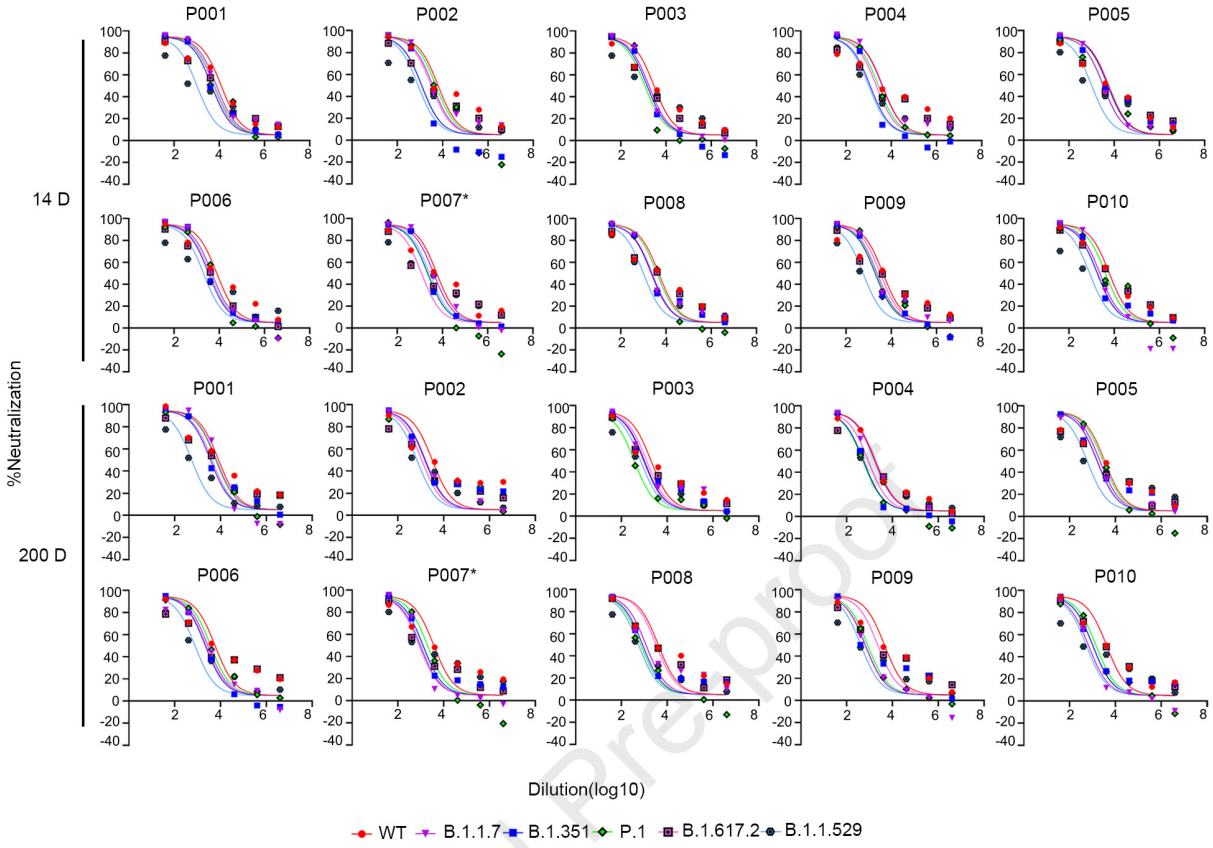

A

Fold change	IC50 of WT / IC50 of Variants									
	WT/B.1.1.7		WT/B.1.351		WT/P.1		WT/B.1.617.2		WT/B.1.1.529	
Volunteer	14 D	200 D	14 D	200 D	14 D	200 D	14 D	200 D	14 D	200 D
P01	1.61	1.23	2.63	2.24	1.91	1.35	2.15	1.93	11.90	14.98
P02	1.73	1.96	5.28	2.11	1.26	1.99	2.01	2.87	7.55	4.65
P03	1.70	1.89	2.02	2.08	2.54	5.39	1.64	1.56	2.02	2.85
P04	1.06	1.11	3.59	3.35	1.53	3.66	1.90	2.09	4.16	3.33
P05	1.77	1.59	1.11	2.12	1.74	1.18	1.70	2.06	5.68	5.79
P06	1.65	2.05	2.29	2.67	1.63	1.55	1.98	2.41	3.88	7.52
P07*	1.38	3.91	2.48	2.97	2.62	1.89	4.73	4.41	2.08	3.74
P08	1.97	3.46	2.12	4.88	1.18	5.77	1.19	1.24	3.33	3.28
P09	1.83	6.94	2.25	6.86	2.08	5.39	1.33	1.97	7.62	10.76
P10	2.61	6.17	3.37	4.00	1.46	2.89	0.97	1.01	7.38	7.58

– +

B